Cellular/Molecular

Tandem Subunits Effectively Constrain $GABA_A$ Receptor Stoichiometry and Recapitulate Receptor Kinetics But Are Insensitive to $GABA_A$ Receptor-Associated Protein

Andrew J. Boileau,[1] Robert A. Pearce,[2] and Cynthia Czajkowski[1]
Departments of [1]Physiology and [2]Anesthesiology, University of Wisconsin-Madison, Madison, Wisconsin 53711

GABAergic synapses likely contain multiple $GABA_A$ receptor subtypes, making postsynaptic currents difficult to dissect. However, even in heterologous expression systems, analysis of receptors composed of α, β, and γ subunits can be confounded by receptors expressed from α and β subunits alone. To produce recombinant $GABA_A$ receptors containing fixed subunit stoichiometry, we coexpressed individual subunits with a "tandem" α1 subunit linked to a β2 subunit. Cotransfection of the γ2 subunit with $\alpha\beta$-tandem subunits in human embryonic kidney 293 cells produced currents that were similar in their macroscopic kinetics, single-channel amplitudes, and pharmacology to overexpression of the γ subunit with nonlinked α1 and β2 subunits. Similarly, expression of α subunits together with $\alpha\beta$-tandem subunits produced receptors having physiological and pharmacological characteristics that closely matched cotransfection of α with β subunits. In this first description of tandem $GABA_A$ subunits measured with patch-clamp and rapid agonist application techniques, we conclude that incorporation of $\alpha\beta$-tandem subunits can be used to fix stoichiometry and to establish the intrinsic kinetic properties of $\alpha1\beta2$ and $\alpha1\beta2\gamma2$ receptors. We used this method to test whether the accessory protein $GABA_A$ receptor-associated protein (GABARAP) alters $GABA_A$ receptor properties directly or influences subunit composition. In recombinant receptors with fixed stoichiometry, coexpression of GABARAP-enhanced green fluorescent protein (EGFP) fusion protein had no effect on desensitization, deactivation, or diazepam potentiation of GABA-mediated currents. However, in $\alpha1\beta2\gamma2S$ transfections in which stoichiometry was not fixed, GABARAP-EGFP altered desensitization, deactivation, and diazepam potentiation of GABA-mediated currents. The data suggest that GABARAP does not alter receptor kinetics directly but by facilitating surface expression of $\alpha\beta\gamma$ receptors.

Key words: **$GABA_A$ receptors; macroscopic kinetics; protein concatamers; tandem subunits; GABARAP; $GABA_A$ receptor trafficking**

Introduction

$GABA_A$ receptors are inhibitory neurotransmitter receptors that are widely distributed in the mammalian CNS. A great number of $GABA_A$ subunits and subunit subtypes have been identified in recent years, including α1–6, β1–3, γ1–3, δ, ϵ, π, and θ (Barnard et al., 1998; Bonnert et al., 1999). These subunits coassemble to form heteropentamers, with the five subunits arranged pseudo-symmetrically around a Cl^- conducting pore. The subtypes α1, β2 (or β1), and γ2 form the most common receptor pentamer, most likely with $2\alpha2\beta1\gamma$ subunit (Benke et al., 1991, 1994; Laurie et al., 1992; Stephenson, 1995). Neuronal constraints on the assembly of particular subunit combinations may be quite strict (Mohler et al., 1995; Hevers and Luddens, 1998), but many combinations are thought to be present in the brain. In transgenic mice with the γ2 subunit "knocked out," conductance levels were reduced and benzodiazepine modulation of GABA-mediated currents was abolished (Gunther et al., 1995), leading the authors to suggest the possibility that receptors composed of only $\alpha+\beta$ subunits were expressed in these knock-out mice. One question raised in recent studies (Baumann et al., 2001, 2002; Boileau et al., 2002, 2003) is whether, even in heterologous expression systems, $GABA_A$ receptors are assembled in pentamers with the expected stoichiometry or arrangement.

Several studies have described differences in pharmacology and kinetics for particular $GABA_A$ subunit combinations, both in oocyte and mammalian cell expression systems (Vicini, 1991; Yeh and Grigorenko, 1995; Vicini, 1999). Comparisons between these studies are sometimes complicated by possible differences in cell type (Mercik et al., 2003), differences in the source of the DNA (e.g., species, subtype), the type of expression vector used, and the speed of agonist application. However, in almost every instance, the receptors examined were transfected or injected in a 1:1:1 α:β:γ ratio. Previous work from our laboratory and others (Boileau and Czajkowski, 1999; Baumann et al., 2001; Boileau et al., 2002, 2003) indicates that transfection or injection of α1, β2, and γ2S subunits in a 1:1:1 α:β:γ ratio can result in a mixture of $\alpha1\beta2$ and $\alpha1\beta2\gamma2S$ receptors.

Here, we constrained stoichiometry by using concatenated "tandem" subunit constructs, with two subunits yoked together by a polyglutamine linker (Im et al., 1995; Baumann et al., 2001).

Received Sept. 5, 2005; revised Oct. 21, 2005; accepted Oct. 21, 2005.

This work was supported by National Institutes of Health Grants MH66406-03 (C.C., A.J.B.) and GM55719 (R.A.P.). We thank Dr. Matt Jones for insightful comments, José L. Mercado for critical reading of this manuscript, and Drs. David Wagner, Jeremy Teissére, and Lee Wheeler for help with tandem construction.

Correspondence should be addressed to Andrew J. Boileau, Department of Physiology, University of Wisconsin-Madison, 601 Science Drive, Madison, WI 53711. E-mail: boileau@wisc.edu.

DOI:10.1523/JNEUROSCI.3751-05.2005

 0270-6474/05/2511219-12$15.00/0

We examined whether incorporation of tandem subunits alters $GABA_A$ receptor kinetic properties and defined the macroscopic kinetic properties of $\alpha1\beta2$ and homogeneous $\alpha1\beta2\gamma2S$ receptors using rapid agonist application to excised outside-out patches from transfected human embryonic kidney 293 (HEK293) cells. Ultra-rapid drug exchanges (100–300 μs) ensured that desensitization and deactivation time constants were not slowed by the exchange time itself, as might occur in the whole-cell configuration (Bianchi and Macdonald, 2002). We also tested for concentration response characteristics, blockade by Zn^{2+}, single-channel conductance, and open probability. In addition, we examined the effect of coexpressing $GABA_A$ receptor-associated protein (GABARAP), an accessory protein known to associate with the $\gamma2$ subunit, on $GABA_A$ receptor kinetics (Barnes, 2000; Nymann-Andersen et al., 2002b).

Materials and Methods

Cell culture and DNA transfection. HEK293 cells (CRL 1573; American Type Culture Collection, Manassas, VA) were maintained in standard culture conditions (37°C, 5% CO_2) and transiently transfected with cDNAs of rat $GABA_A$ receptor subunits $\alpha1$, $\beta2$, and $\gamma2S$ as described previously (Boileau et al., 2003) or $\gamma2L$ (generously provided by Dr. David Weiss, University of Alabama at Birmingham, Birmingham, AL). The culture media consisted of minimal essential medium with Earle's salts (Invitrogen, Carlsbad, CA) containing 10% fetal bovine serum (Harlan Bioproducts for Sciences, Indianapolis, IN). Cells were plated in 35 mm culture dishes 48–96 h before transient transfection. cDNAs for $GABA_A$ receptor subunits were subcloned into the multiple cloning site of the mammalian expression vector pCEP4 (Invitrogen) for transfection. Untranslated regions from the GenBank databases both upstream ($\geq$44 bases) and downstream ($\geq$100 bases) of the open reading frame were included in $\alpha1$, $\beta2$, and $\gamma2$ cDNAs, as were the native Kozak recognition sequences. Cells were cotransfected at 70–90% confluence using Lipofectamine 2000 (Invitrogen). Generally, we used 200 ng each of pCEP4-$\alpha1$ and pCEP4-$\beta2$ and varied the weight ratio of pCEP4-$\gamma2$. The GABARAP-enhanced green fluorescent protein (EGFP) fusion protein (generously provided by Dr. Lotfi Ferhat, Institut de Neurobiologie de la Méditerranée, Institut National de la Santé et de la Recherche Médicale U29, Marseilles, France) was constructed by fusing cDNA encoding rat GABARAP with EGFP in the pEGFP-N1 vector (Clontech, Mountain View, CA) and cotransfected at a $\geq$6:1 molar ratio to the $\alpha1$ subunit. Cells were cotransfected with EGFP (Clontech) either with pEGFP-N1, EGFP subcloned into pCEP4, or the pCEP4-GABARAP-EGFP construct and identified as transfected using a mercury arc lamp and a wild-type (wt) GFP filter cube (HQ:GFP 41014; Chroma Technology, Rockingham, VT). Cells were replated on 12 mm circle cover glass in culture trays with four 16 mm wells (Fisher Scientific, Pittsburgh, PA) 4–8 h after transfection, incubated for 14–18 h at 37°C, and then moved to a separate CO_2 chamber (31°C; 7% CO_2) with no observable differences in kinetic measurements compared with cells left at 37°C. The episomal replication of the pCEP4 vector and the lowered growth temperature allowed for recording from passaged transfected cells for up to several days. All recordings were made at room temperature.

Tandem design and subcloning. Tandem subunits with rat $\alpha1$ cDNA linked at the 3′-end to the 5′-end of rat $\beta2$ subunit cDNA were patterned after $\alpha6$-$\beta2$ tandem subunits constructed by Im et al. (1995). Briefly, one oligonucleotide was generated with codons for nine additional glutamines $(5'\text{-CAG-}3')_9$ beyond the final glutamine of the $\alpha1$ sequence, followed by sequence corresponding to the 5′ beginning of the $\beta2$ sequence, including the entire signal peptide sequence. This oligonucleotide was used in conjunction with a downstream $\beta2$ oligonucleotide to create a PCR product (Expand; Roche Diagnostics, Indianapolis, IN). PCR was also performed separately with an upstream $\alpha1$ oligonucleotide paired with a downstream oligonucleotide designed to remove the $\alpha1$ stop codon and add the reverse complement of the nine glutamine sequence used for the $\beta2$ PCR. The "$\alpha1+9Q$" and "$9Q+\beta2$" PCR products were purified (HiPure PCR Product Purification Kit; Roche Diagnostics), mixed, annealed, and extended by PCR to create a cassette with the 9Q sequence joining the $\alpha1$ sequence to the $\beta2$ start codon. This cassette was then subcloned into existing restriction sites in $\alpha1$ and $\beta2$ sequence (*Bam*HI and *Bsp*EI, respectively) in a construct wherein the $\alpha1$ and $\beta2$ subunits had previously been subcloned, in register, in the plasmid vector pBluescript SK- (Stratagene, La Jolla, CA). After replacement of the intervening sequence with the cassette, the tandem $\alpha1$-$\beta2$ ($\alpha\beta$tan) sequence was then subcloned into the expression vector pCEP4.

Biochemical detection of tandem subunits. HEK cells were grown on 100 mM culture dishes and transfected with $\alpha1_{FLAG}$ or $\alpha1_{FLAG}$-β tandem (20 μg) using a standard CaHPO4 precipitation method (Graham and van der Eb, 1973). The subunits all contained the FLAG epitope sequence (DYKDDDDK) inserted between the sixth and seventh amino acid of the mature $\alpha1$ subunit.

Forty-eight hours after transfection, intact cells were washed with ice-cold PBS (2.7 mM KCl, 1.5 mM KH2PO4, 0.5 mM MgCl2, 137 mM NaCl, and 14 mM Na2HPO4, pH 7.1). Sulfhydryl groups were blocked by incubating the cells with 10 mM *N*-ethylmaleimide (NEM) in PBS (20 min, room temperature). Cells were solubilized (2 h, 4°C) in lysis buffer (1% Triton X-100, 50 mM Tris-HCl, 150 mM NaCl, 5 mM EDTA, pH 7.5) supplemented with protease inhibitors (0.5 mg/ml Pefabloc, 1 μg/ml pepstatin, 1 μg/ml leupeptin; Roche Molecular Biochemicals) and 10 mM NEM. Lysates were cleared by centrifugation (16,000 × *g*; 10 min; 4°C).

The FLAG-tagged $GABA_A$ receptor subunits were immunopurified from the cell lysates by incubating (2 h, 4°C, rotating) with 50 μl of FLAG-agarose beads (Sigma-Aldrich, St. Louis, MO). The samples were then centrifuged (16,000 × *g*, 10 min, 4°C), and the beads were washed four times with 1 ml of wash buffer (0.1% Triton X-100, 150 mM NaCl, 5 mM EDTA, and 50 mM Tris-Cl, pH 7.5) and once with 1 ml of 25 mM Tris-Cl. The FLAG-tagged subunits were eluted from the beads with 100 μl of 400 μg/ml FLAG peptide in wash buffer (1 h; 4°C rotating). After the incubation, the samples were centrifuged (16,000 × *g*; 10 min; 4°C), the eluate collected and denatured with 2× Laemmli Sample Buffer (3% SDS, 0.6 M sucrose, 0.325 M Tris-HCl, pH 6.8, 10 mM DTT).

Protein samples were run on 7.5% SDS-polyacrylamide gels and transferred to nitrocellulose membranes (0.45 μm). The nitrocellulose membrane was washed three times with 20 mM Tris-HCl, 500 mM NaCl, pH 7.5 (TBS); blocked for 1 h at room temperature with 0.5% low-fat powdered milk in TBS; and washed three times with 0.5% Tween 20 in TBS (TTBS). Blots were incubated in primary antibody diluted in TTBS plus 0.5% powdered milk (5 μg/ml M2 anti-FLAG; Sigma-Aldrich) overnight at 4°C and then washed four times in TTBS. Blots were then incubated in secondary antibody (horseradish peroxidase conjugated goat anti-mouse IgG; Pierce, Rockford, IL) for 1 h at room temperature and then washed six times with TTBS and before developing with Super Signal ECL substrate (Pierce).

Drug application and recording. Solutions were applied to excised outside-out patches using a four-barrel square glass application pipette (Vitrocom, Mountain Lakes, NJ) connected to a piezoelectric stacked translator (Physik Instrumente, Costa Mesa, CA). The glass was connected to solution reservoirs (30 ml plastic syringes) via six-way, low pressure, zero dead volume, Teflon selector valves (Varian, Palo Alto, CA), with Teflon tubing for the valve inlets and thin-walled polyimide tubing (Cole-Parmer, Vernon Hills, IL) for the outlets and sealed with Sylgard 184 (Dow-Corning, Midland, MI) and/or epoxy resin. Tygon tubing, as we and others (D. A. Wagner, M. P. Goldschen, and M. V. Jones, unpublished observations) have observed, can result in kinetic changes that resemble use-dependent channel block for $GABA_A$ receptors (data not shown), so we avoided its use. By minimizing dead volumes, solutions flowing from the application pipette could be completely exchanged in ~30 s, allowing concentration–response relationships to be obtained from single patches. The voltage input driven by pClamp7 software (Molecular Dynamics, Foster City, CA) to the high-voltage amplifier (Physik Instrumente, Costa Mesa, CA) used to drive the stacked translator was filtered at 90 Hz using an 8-pole Bessel Filter (Frequency Devices, Haverhill, MA) to reduce oscillations arising from rapid accel-

eration of the pipette. The open-tip solution exchange time was estimated using a solution of lower ionic strength in the drug barrel after experiments were completed. Open tip solution exchange times of 100–300 μs (τ) were typically achieved. For excised patches, this has been shown to correlate well with drug application times (Trussell and Fischbach, 1989).

The recording chamber was perfused continuously with HEPES-buffered saline containing the following (in mM): 135 NaCl, 5.4 KCl, 1 $MgCl_2$, 1.8 $CaCl_2$, 5 HEPES, pH 7.2. This standard saline was also used as the "control" solution in the rapid application pipette. Recording pipettes were filled with the following (in mM): 129 KCl, 9 NaCl, 5 EGTA, 10 HEPES, 4 $MgCl_2$, pH 7.2. The Cl^- equilibrium potential across the patch was ~0 mV. GABA solutions were prepared daily from powder and diluted to desired concentrations in the same control/bath solution. Recordings were performed at room temperature (22–25°C) on the stage of a Nikon (Tokyo, Japan) Diaphot microscope.

Recording electrodes were fabricated from KG-33 glass (Garner Glass, Claremont, CA) using a multistage puller (Flaming-Brown model P-97; Sutter Instruments, Novato, CA) and coated with Sylgard to reduce electrode capacitance for single-channel patches. The tips were fire polished. Open tip electrode resistance was typically 3–7 MΩ when filling with standard recording solution. Most recordings were obtained at a holding potential of −40 mV, except when otherwise specified, using a low-noise patch amplifier (Axopatch 200A; Molecular Devices). Data were low-pass filtered at 2–5 kHz using amplifier circuitry, sampled at 5–10 kHz, and stored on-line using pClamp 7 software.

Data analysis. Axograph, pClamp (Molecular Devices), ORIGIN (Microcal Software, Northampton, MA), Excel (Microsoft, Redmond, WA), and Prism (Graphpad, San Diego, CA) were used for data acquisition and analysis. Statistical comparisons were made using one-way ANOVA with Dunnett's posttest for significance of difference between transfection conditions, or Bonferroni's multiple comparison test for paired transfections with or without GABARAP-EGFP (Graphpad).

Desensitization and deactivation of currents were fit with multiple exponentials (plus a nonzero constant for desensitization). All desensitization curves were fit to 20 s GABA pulses (10 mM), which appeared sufficiently long to generate good fits with four time constants. Deactivation was best fit with two or three time constants, using either Chebyshev or simplex SSE algorithms, as determined by visual inspection using Axograph. Intervals empirically determined to reduce run-down between pulses were longer for $\alpha1\beta2$ (or $\alpha\beta$tan+$\alpha1$) versus $\alpha1\beta2\gamma2S$ or ($\alpha\beta$tan+$\gamma2S$) transfections: intervals were 40 versus 15 s (for 5 ms pulses at 1–10 mM GABA), 50 versus 20 s (for 20 ms pulses), 90 versus 45 s (for 200 ms pulses), 210 versus 120 s (for 2 s pulses), and 300 versus 210 s (for 20 s pulses), respectively. Some of these intervals may exceed the minimum requirement for run-down reduction. For long protocols, high-concentration GABA solutions were turned off between pulses to reduce accumulation in the bath. The contribution of individual components in multiexponential fits was expressed as a percentage amplitude (%A), calculated as $A_n/(\Sigma A_n + c) \times 100\%$, where c is the constant from the exponential fit for desensitization ($c = 0$ for deactivation). Weighted time constants were calculated as $\tau_w = \Sigma(\tau_n \times A_n)/\Sigma A_n$.

GABA concentration–response curves were generated from tests of three or more excised patches. Generally, concentrations were tested starting from lowest to highest and then in reversed order in the same patch. Concentration–response curves for GABA were fitted with the equation $I = I_{max}/[1 + (EC_{50}/A)^n]$, where A is the agonist concentration, EC_{50} the concentration of GABA eliciting half-maximal current amplitude, I_{max} is the maximal current amplitude, I is the current amplitude, and n is the Hill coefficient. I_{max} was set at a concentration 10-fold higher than the apparent peak response at lower concentrations, and this maximal concentration was applied between each lower concentration step and used as the scale for the previous pulse of lower concentration. Intervals between pulses were 60 s (twice the interval needed for a full solution exchange from one concentration to another), and pulse durations ranged from 2 s durations for the largest dilution of agonist used for

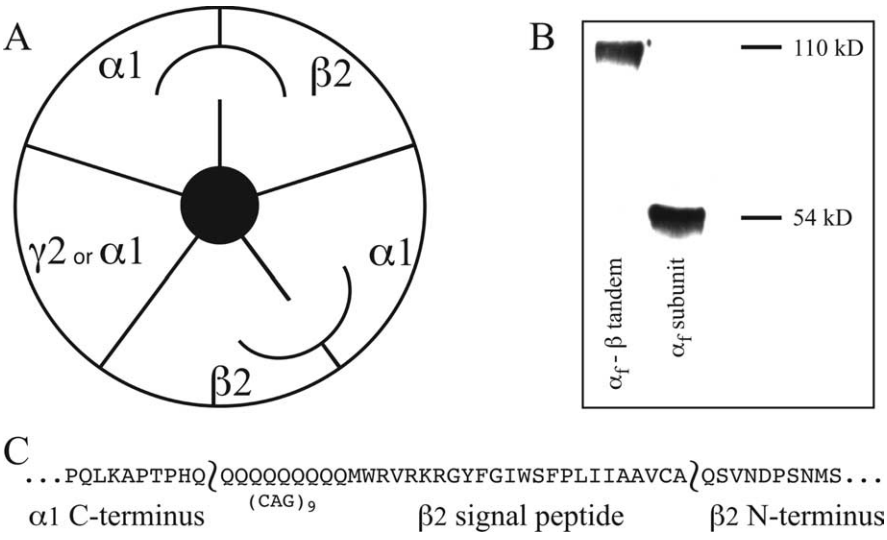

Figure 1. Tandems and Western blot. ***A***, Tandem subunits (depicted with arc linkage) were expressed alone or with free $\alpha1$, $\beta2$, or $\gamma2S$ subunits in a 2:1 ratio. Only $\alpha1$ and $\gamma2$ coexpression gave functional expression. ***B***, The α_{FLAG}-β tandem subunit is stable. Representative Western blot from cells expressing α_{FLAG} and α_{FLAG}-β subunits probed with anti-FLAG antibody. The immunoreactive band at 54 kDa corresponds to the α_{FLAG} monomer, and the band at 110 kDa corresponds to α_{FLAG}-β concatamerized dimer. In cells expressing the α_{FLAG}-β tandem subunit, no smaller immunoreactive molecular weight bands were detected, indicating that the tandem subunit is not appreciably breaking down. Similar results were obtained in three experiments. ***C***, Peptide map of the linker between the $\alpha1$ and $\beta2$ subunits in the $\alpha\beta$ tandem. Nine additional glutamine residues were added using a CAG repeat, and the $\beta2$ signal peptide sequence was retained in the construct.

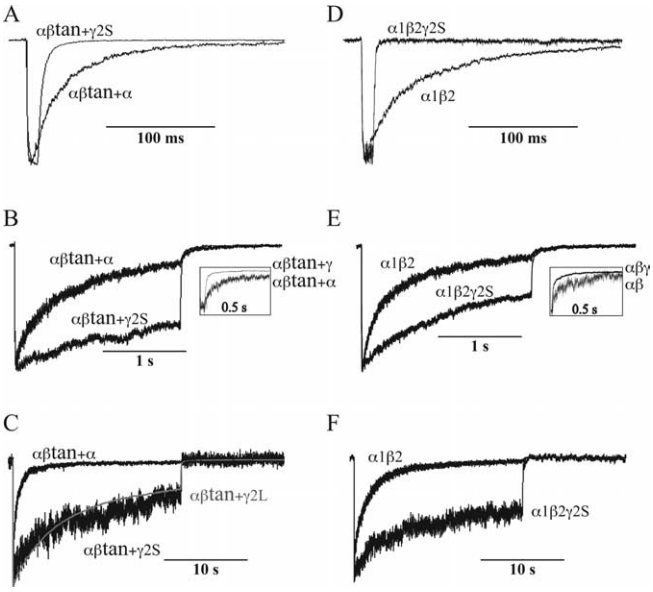

Figure 2. Current traces comparing receptors formed from different transfections: $\alpha1\beta2$, $\alpha\beta$tan+$\alpha1$, $\alpha1\beta2\gamma2S$ 1:1:10, $\alpha\beta$tan+$\gamma2S$, and $\alpha\beta$tan+$\gamma2L$. GABA (10 mM) pulse durations were 20 ms (top row, ***A***, ***D***), 2000 ms (middle row, ***B***, ***E***) and 20,000 ms (bottom row, ***C***, ***F***). Differences in desensitization are more clearly seen in longer (2000 and 20,000 ms) pulses, and comparisons of deactivation are visible in short (20 ms) traces and in longer traces when normalized to the current at the end of the pulse (middle row, insets). One example of $\alpha\beta$tan+$\gamma2L$ is shown for comparison in ***C*** (gray).

Table 1. Desensitization: time constants (s) from excised patches

20 s pulse	τ1	%	τ2	%	τ3	%	τ4	%	τ(w)	n
α1β2	0.024 ± 0.002	12 ± 6	0.13 ± 0.01	18 ± 15	1.04 ± 0.47	57 ± 14	4.0 ± 1.0	10 ± 4	1.1 ± 0.4	4
+GABARAP	0.024 ± 0.001	14 ± 9	0.36 ± 0.18	23 ± 18	1.15 ± 0.69	42 ± 18	3.5 ± 1.0	19 ± 6	1.1 ± 0.2	4
αβtan+α1	0.024 ± 0.001	26 ± 3	0.22 ± 0.13	20 ± 17	0.62 ± 0.22	39 ± 18	4.9 ± 1.9	14 ± 6	1.0 ± 0.5	3
α1β2γ2S 1:1:0.5	0.006 ± 0.003	8 ± 5	0.17 ± 0.17	26 ± 23	1.27 ± 0.79	39 ± 19	3.9 ± 1.6	24 ± 17	1.5 ± 0.8	4
+GABARAP	0.025 ± *	2 ± *	0.39 ± 0.16	4 ± 5	1.14 ± 0.26	50 ± 31	6.0 ± 1.5	30 ± 13	3.1 ± 1.7	4
α1β2γ2S 1:1:1	0.012 ± 0.008	8 ± 7	0.27 ± 0.11	19 ± 9	1.27 ± 0.39	55 ± 14	5.7 ± 3.1	14 ± 13	1.9 ± 0.7	7
α1β2γ2S 1:1:10					1.41 ± 0.33	33 ± 26	6.3 ± 2.4	44 ± 11	4.4 ± 1.9	5
+GABARAP					1.10 ± 0.46	45 ± 17	7.2 ± 2.4	38 ± 14	4.4 ± 1.5	7
αβtan+γ2S					1.07 ± 0.03	21 ± 3	6.2 ± 1.6	70 ± 7	5.7 ± 1.6	5
+GABARAP					1.38 ± 0.63	19 ± 9	5.2 ± 1.1	68 ± 12	4.3 ± 1.1	4
αβtan+γ2L					1.16 ± 0.27	19 ± 8	7.2 ± 0.7	56 ± 15	5.7 ± 0.7	4

a given receptor type, down to 30 ms for the highest concentrations. A full curve from lowest to highest concentration and then back down required ~30 min to acquire. Data are reported as mean ± SEM. Patches with >10% run-down in peak current were discarded.

Zinc blockade tests were performed as follows: patches were tested with 200 ms pulses of 1 mM GABA, and peak current was measured for three or more trials to assess run-down. Patches exhibiting >10% run-down were discarded. Patches were then preincubated for ≥30 s in control solution containing 30 μM $ZnCl_2$ and then exposed to 1 mM GABA plus 30 μM $ZnCl_2$, and peak current was measured in this condition. Cells were then washed back into control solutions to recover from Zn^{2+} block and retested. If the posttest peaks were decreased by >10% from the original control peaks, the test was repeated for that patch or discarded. Percentage block was calculated as follows: 1 − (peak current in Zn^{2+})/(peak current in control) × 100%.

Potentiation of I_{GABA} by diazepam (DZ) was performed as follows: patches were exposed repeatedly to a low concentration of GABA (3 μM) for 500 ms until a stable current level was achieved. Subsequently, we preincubated ≥30 s with control solution plus 1 μM DZ. Finally, we applied 500 ms duration pulses of 3 μM GABA plus 1 μM diazepam until a stable current level was achieved. Potentiation was calculated from peak currents before and during diazepam exposure using the equation $I_{GABA+DZ}/I_{GABA} - 1$.

Mean-variance experiments to estimate open probability (P_o) were performed by averaging 30–150 short GABA pulses from a single excised patch, for three or more patches for a given transfection type (Traynelis et al., 1993). GABA concentration was 1 mM, and 20 ms pulses were taken with an interval determined to reduce or eliminate the run-down caused by accumulation of desensitization for a particular subunit combination. Consecutive traces were then averaged, and ensemble variance was calculated for all points from the peak to the end of the 1.6 s sweeps. Data were plotted as mean versus ensemble variance and fitted to the equation $\sigma^2 = iI - I^2/N + c$, where σ^2 is the variance, i is the unitary conductance, I is the mean current, N is the number of ion channels, and c is the y-axis intercept. P_o is estimated by dividing the rightmost value of the data (equivalent to iNP_o) by the maximum value generated by the parabolic curve fit, where the curve intercepts the mean (x) axis at iN.

Single-channel chord conductances were measured from single openings observed in deactivating currents following saturating (10 mM) GABA pulses. Identified openings of >0.5 ms (approximately two times the measured system dead time) duration were sectioned out of longer recordings and grouped, and amplitude histograms were fitted to multiple Gaussian distributions to determine amplitudes. Rare double openings were discarded from additional analysis, as were occasional openings corresponding to small (<5 pS) conductances. Mean amplitude (pA) was then plotted against the voltage (mV), and chord conductance was calculated from the slope. In patches with very few or one channel opening, data were gathered from patches under continuous exposure to 1–10 mM GABA, and clusters of openings were analyzed for amplitudes in the same manner. Data presented are mean ± SEM for a minimum of four patches per transfection mixture.

Modeling. Model current data were generated using the chemical-kinetic modeling plug-in in Axograph. Initial values for k_{on}, k_{off}, β, and α rates were adapted from other models of GABA$_A$ receptor kinetics (Jones and Westbrook, 1995; Hinkle and Macdonald, 2003), with an unbound closed state (U), singly liganded (B1) and doubly liganded (B2) states, and an open state for each bound state (O1, O_2, respectively). Several state connection schemes were compared, with desensitized (D) states progressing from B1, or with some D states connected to one another. A simplified scheme with all D states connected to B2 was sufficient and robust. Based on the desensitization seen in pulses of 20 s, 10 mM GABA, four D states connected to B2 was optimized for receptors formed from α-β tandem subunits plus α1, and two D states were required to model receptors expressed using α-β tandem plus γ2S. This model approximates EC_{50}, relative open probability, desensitization, and deactivation characteristics of each receptor type.

A model for benzodiazepine potentiation was created using the relative potentiation expected with varying mixtures of αβ and αβγ receptors. Maximal diazepam potentiation was modeled as in the experimental protocol at 3 μM GABA plus 1 μM diazepam. The EC_{50} values for αβ and αβγ receptors determined experimentally were factored in, as was the open probability for αβγ receptors (0.69). The open probability for αβ receptors was estimated at 0.45, slightly lower than the values we determined for some αβ transfections (see Results) but also intermediate to estimates derived from first latency analysis (Burkat et al., 2001). Adjustments were also made for the relative amount of subconductance compared with main conductance for each receptor type (Angelotti and Macdonald, 1993). Minimal potentiation was set at zero for αβ receptors, and maximal potentiation and 95% confidence intervals were derived from αβtan+γ2 transfection data.

Results

We characterized receptors formed using a tandem α1-β2 subunit to constrain subunit stoichiometry and expression (αβtan) (Fig. 1). The tandem subunit was expressed in a 2:1 ratio with either free α1, free β2, or free γ2 subunits, and we compared the kinetic properties to receptors formed using α1+β2 subunits expressed in 1:1 ratio and α1+β2+γ2 subunits expressed in 1:1:10 and 1:1:1 ratios. We first tested whether expression of the tandem α1-β2 subunit cDNA resulted in the synthesis of a full-length tandem subunit (Fig. 1). Western analysis showed tandem concatamer protein of appropriate size (110 K_d dimer) with no apparent degradation products, suggesting that tandems do not break into or express single subunits that might incorporate into receptors. No current was detected with expression of tandems alone or tandems plus free β2 subunits (data not shown), again suggesting that incomplete incorporation of tandem subunits was not occurring (e.g., one of the two subunits does not "loop out" of the receptor). Also, if the N terminus of the tandem subunits were degraded, leaving a full-length β2 subunit, it would not express functional receptors with other tandems. Figure 2*A–C* shows current traces from transfections with αβtan+α1 and αβtan+γ2S. For comparison, Figure 2*D–F* shows typical

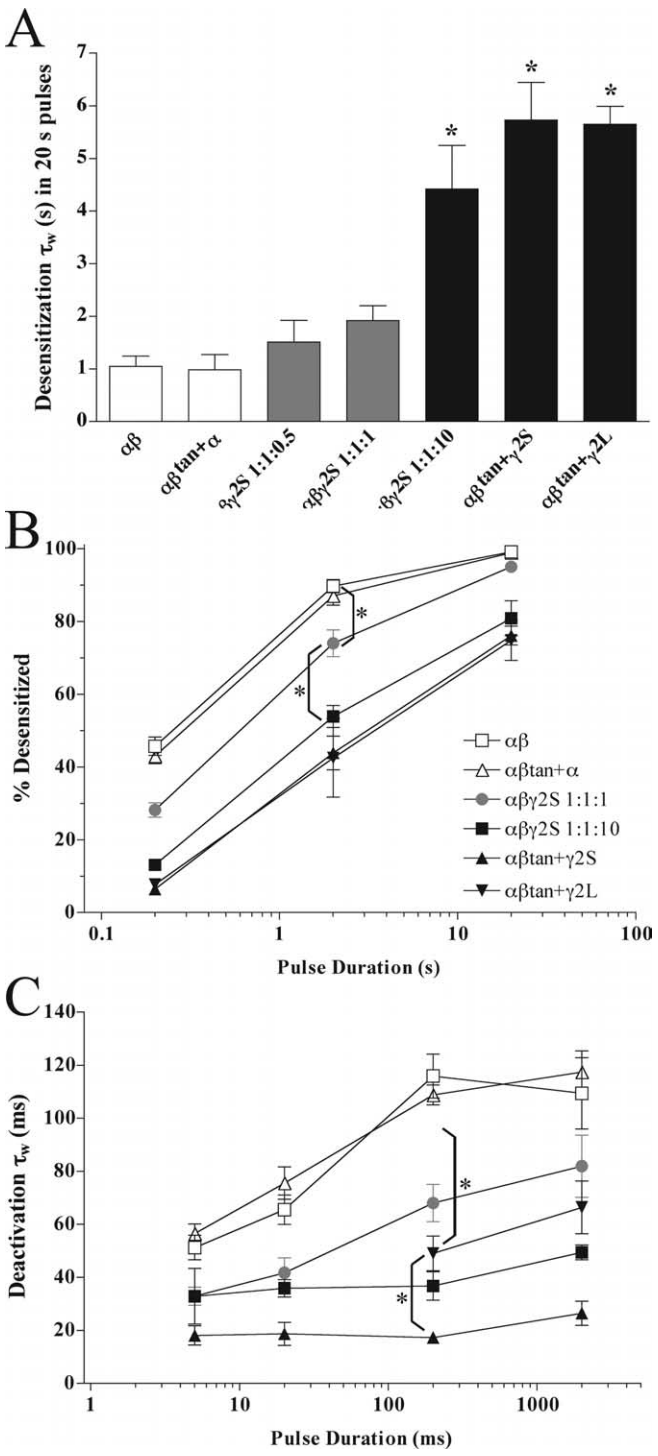

Figure 3. Desensitization and deactivation profiles for different transfections. ***A***, Weighted desensitization time constants (τ_w) differ between $\alpha1\beta2$ or $\alpha\beta$tan+$\alpha1$ transfections (open bars) and $\alpha1\beta2\gamma2S$ 1:1:10 or $\alpha\beta$tan+$\gamma2S$ or $\gamma2L$ transfections (black bars). Transfections with $\alpha\beta\gamma$ in a 1:1:0.5 or 1:1:1 ratio (gray bars) result in intermediate τ_w. Statistical comparisons reveal that $\alpha\beta$ and $\alpha\beta$tan+$\alpha1$ transfections differ significantly from $\alpha\beta\gamma$ 1:1:10 and $\alpha\beta$tan+$\gamma2S$ transfections (*$p < 0.001$) but not from $\alpha\beta\gamma$ 1:1:0.5 or 1:1:1. $\alpha\beta\gamma$ 1:1:10 and $\alpha\beta$tan+$\gamma2S$ weighted time constants are not significantly different from each other. Data are mean ± SEM. ***B***, Comparison of the percentage of the peak current remaining at the ends of 10 mM GABA pulses of varying length. Percentage desensitization was calculated as follows: 1 − (current amplitude at pulse end/peak current) × 100%. Transfections with $\alpha1\beta2\gamma2S$ 1:1:1 (gray circles) result in values intermediate to $\alpha1\beta2$ and $\alpha\beta$tan+$\alpha1$ (open symbols) versus $\alpha1\beta2\gamma2S$ 1:1:10, $\alpha\beta$tan+$\gamma2S$, and $\alpha\beta$tan+$\gamma2L$ transfections (closed symbols). This difference is most clearly observed at the ends of 2 s pulses (*$p < 0.001$ compared with $\alpha1\beta2\gamma2S$ 1:1:1 transfections). Data are mean ± SEM. ***C***, Weighted deactivation time constants for $GABA_A$ current traces directly comparing excised patches from transfections of free $\alpha1+\beta2$ subunits only ($\alpha\beta$), to transfections of $\alpha1$, $\beta2$, and $\gamma2$ in a 1:1:10 ratio. In both desensitization and deactivation, transfections with $\alpha\beta$tan+$\alpha1$ displayed characteristics indistinguishable from $\alpha1\beta2$ receptors (Fig. 2, compare *A–C* and *D–F*), and transfections of $\alpha\beta$tan+$\gamma2S$ subunits yielded currents similar to $\alpha1$:$\beta2$:$\gamma2$ 1:1:10. For $\alpha\beta$tan+$\alpha1$ or $\alpha1\beta2$, desensitization was much greater and deactivation was slower than for transfections with $\gamma2$ subunits.

For 20 s duration GABA pulses, two time constants were required to fit the desensitization for $\alpha\beta$tan+$\gamma2$ or $\alpha1\beta2\gamma2S$ 1:1:10 transfections, whereas four were required for either $\alpha\beta$tan+$\alpha1$ or $\alpha1\beta2$ receptors (Table 1). In two of 25 patches from $\alpha1\beta2\gamma2S$ 1:1:10 transfections, a small faster component of desensitization could be observed (data not shown). Weighted time constants for desensitization and deactivation for the receptors studied are presented graphically in Figure 3. The weighted desensitization time constants for $\alpha\beta$tan+$\gamma2S$ and $\alpha1\beta2\gamma2S$ 1:1:10 transfections were significantly different from $\alpha1\beta2$ transfections ($p < 0.001$), but $\alpha\beta$tan+$\alpha1$, $\alpha1\beta2\gamma2S$ 1:1:0.5, and $\alpha1\beta2\gamma2S$ 1:1:1 were not (Fig. 3*A*). Figure 3*B* depicts the differences in the extent of desensitization for the receptors studied with 10 mM GABA pulses of varying duration. At the end of a 200 ms, 2 s, or 20 s GABA pulse, the extent of desensitization in $\alpha\beta$tan+$\alpha1$ transfections was not significantly different from $\alpha\beta$ transfections, and the same measure in $\alpha\beta$tan+$\gamma2$ versus $\alpha1\beta2\gamma2S$ 1:1:10 transfections were indistinguishable. However, the extent of desensitization in $\alpha1\beta2\gamma2S$ 1:1:1 transfections was significantly greater than either $\alpha1\beta2\gamma2S$ 1:1:10 or $\alpha\beta$tan+$\gamma2S$ transfections for all three pulse durations ($p < 0.05$). Furthermore, the extent of desensitization in $\alpha1\beta2\gamma2S$ 1:1:1 transfections also differed from $\alpha\beta$tan+$\alpha1$ and $\alpha1\beta2$ transfections at the end of a 2 s GABA pulse ($p < 0.05$) (Fig. 3*B*). Using a longer $\gamma2$ splice variant ($\gamma2L$) with an 8 amino acid insertion in the cytoplasmic loop between transmembrane segments M3 and M4 (Kofuji et al., 1991) in place of $\gamma2S$ subunits coexpressed with $\alpha\beta$tan yielded similar overall kinetics, with the exception of measurably slower deactivation (Benkwitz et al., 2004) (Figs. 2*F*, 3; Table 2).

Slower deactivation of $\alpha\beta$tan+$\alpha1$ and $\alpha1\beta2$ receptors was also readily seen for short GABA pulses (20 ms) (Fig. 2*A*,*D*) and at the ends of longer pulses (2 s) (Fig. 2*B*,*E*, insets). We generally required two time constants to fit deactivation for $\alpha\beta$tan+$\alpha1$ and $\alpha1\beta2$ receptors and three for $\alpha\beta$tan+$\gamma2S$ and $\alpha1\beta2\gamma2S$ 1:1:10 receptors (Table 2). The amplitude of the slowest time constant was larger in short GABA pulse durations for $\alpha1\beta2$ receptors compared with γ-containing receptors. Note that the value of τ_3 tends to increase with GABA pulse duration for all receptor combinations (Table 2). For 200 ms pulses, weighted deactivation time constants for $\alpha1\beta2\gamma2S$ 1:1:1 transfections were significantly different from any of the other transfection types depicted (Fig. 3*C*) ($p < 0.001$), intermediate to $\alpha1\beta2$, and $\alpha1\beta2\gamma2S$ 1:1:10 transfections. There was no significant difference between $\alpha1\beta2\gamma2S$ 1:1:10 and $\alpha\beta$tan+$\gamma2S$ transfections at any pulse duration in this measure, but the apparent trend of slower deactivation in $\alpha1\beta2\gamma2S$ 1:1:10 transfections compared with

←

subunit transfections. Deactivation time constants (τ_w) for $\alpha1\beta2$ and $\alpha\beta$tan+$\alpha1$ transfections (open symbols) and $\alpha1\beta2\gamma2S$ 1:1:10, $\alpha\beta$tan+$\gamma2S$, and $\alpha\beta$tan+$\gamma2L$ transfections (closed symbols). Transfections with $\alpha1\beta2\gamma2S$ 1:1:1 (gray symbols) result in intermediate time constants in pulses of 200 or 2000 ms (*$p < 0.01$ compared with $\alpha1\beta2\gamma2S$ 1:1:1 transfections). Data are mean ± SEM. Components of each weighted time constant are listed in Tables 1 and 2.

Table 2. Deactivation: time constants (ms) from excised patches

	τ1	%	τ2	%	τ3	%	τ(w)	n
≤5 ms pulse								
α1β2			16 ± 5	59 ± 14	105 ± 17	41 ± 14	51 ± 9	4
αβtan+α1			22 ± 9	50 ± 16	97 ± 32	50 ± 16	57 ± 7	4
α1β2γ2S 1:1:1	7 ± 5	27 ± 20	24 ± 4	40 ± 31	76 ± 25	32 ± 22	33 ± 9	7
α1β2γ2S 1:1:10	6 ± 3	49 ± 20	50 ± 24	49 ± 23	129 ± 77	2 ± 4	33 ± 18	3
αβtan+γ2S	4 ± 3	69 ± 29	23 ± 2	24 ± 29	124 ± 37	7 ± 7	18 ± 8	5
20 ms pulse								
α1β2			29 ± 3	54 ± 3	110 ± 25	46 ± 3	65 ± 10	3
+GABARAP			33 ± 6	33 ± 14	112 ± 41	67 ± 14	54 ± 6	3
αβtan+α1			34 ± 9	71 ± 11	191 ± 71	29 ± 11	76 ± 11	3
α1β2γ2S 1:1:0.5			33 ± 9	89 ± 4	130 ± 61	11 ± 4	43 ± 13	5
+GABARAP			39 ± 5	91 ± 7	101 ± 13	9 ± 7	44 ± 3	3
α1β2γ2S 1:1:1	5 ± 3	10 ± 14	30 ± 15	71 ± 19	113 ± 64	19 ± 17	42 ± 19	12
α1β2γ2S 1:1:10	4 ± 3	39 ± 26	32 ± 16	42 ± 18	134 ± 39	19 ± 14	36 ± 7	4
+GABARAP	7 ± 6	37 ± 30	30 ± 8	62 ± 30	131 ± 53	1.6 ± 1.9	23 ± 10	7
αβtan+γ2S	4 ± 3	38 ± 52	21 ± 2	60 ± 52	80 ± 7	1.8 ± 0.01	19 ± 8	3
+GABARAP	4 ± 2	70 ± 20	32 ± 21	25 ± 18	140 ± 75	4.9 ± 2.1	13 ± 5	6
200 ms pulse								
α1β2			46 ± 18	58 ± 17	253 ± 100	42 ± 17	116 ± 29	12
+GABARAP			41 ± 11	37 ± 6	208 ± 76	63 ± 6	101 ± 30	7
αβtan+α1			37 ± 18	45 ± 15	174 ± 35	55 ± 15	109 ± 15	16
α1β2γ2S 1:1:0.5			34 ± 10	87 ± 16	273 ± 136	13 ± 16	57 ± 14	13
+GABARAP			35 ± 8	88 ± 17	214 ± 128	12 ± 17	47 ± 11	5
α1β2γ2S 1:1:1	15 ± 8	40 ± 30	51 ± 24	44 ± 28	281 ± 189	16 ± 16	68 ± 34	22
α1β2γ2S 1:1:10	6 ± 4	43 ± 27	53 ± 31	49 ± 25	249 ± 90	8 ± 9	37 ± 19	12
+GABARAP	6 ± 3	39 ± 31	30 ± 5	51 ± 34	227 ± 117	10 ± 11	32 ± 12	6
αβtan+γ2S	4 ± 3	49 ± 32	28 ± 16	47 ± 32	182 ± 102	4 ± 3	17 ± 7	12
+GABARAP	3 ± 2	72 ± 29	12 ± 8	16 ± 23	70 ± 22	12 ± 7	12 ± 7	3
αβtan+γ2L			29 ± 12	90 ± 2	229 ± 133	10 ± 2	49 ± 13	4
2 s pulse								
α1β2			33 ± 15	54 ± 32	313 ± 48	46 ± 32	109 ± 30	5
+GABARAP			40 ± 11	44 ± 11	220 ± 83	56 ± 11	113 ± 29	4
αβtan+α1			24 ± 14	60 ± 17	280 ± 94	40 ± 17	117 ± 14	3
α1β2γ2S 1:1:0.5			42 ± 14	89 ± 9	502 ± 275	11 ± 9	81 ± 24	11
+GABARAP			27 ± 5	73 ± 22	194 ± 122	27 ± 22	53 ± 11	5
α1β2γ2S 1:1:1	14 ± 7	33 ± 40	40 ± 12	41 ± 36	237 ± 130	27 ± 18	82 ± 47	16
α1β2γ2S 1:1:10	5 ± 3	42 ± 22	42 ± 4	47 ± 28	348 ± 138	11 ± 9	49 ± 6	5
+GABARAP	8 ± 7	43 ± 14	54 ± 25	51 ± 13	299 ± 82	5 ± 5	33 ± 14	5
αβtan+γ2S	5 ± 3	63 ± 36	46 ± 12	34 ± 36	378 ± 199	4 ± 4	26 ± 12	7
+GABARAP	5 ± 2	64 ± 16	54 ± 10	32 ± 16	322 ± 70	3 ± 1	31 ± 5	3
αβtan+γ2L			38 ± 10	88 ± 7	240 ± 78	12 ± 7	66 ± 17	3
20 s pulse								
α1β2γ2S 1:1:0.5			48 ± 21	88 ± 6	1022 ± 758	12 ± 6	158 ± 80	4
+GABARAP	28 ± 7	63 ± 32	116 ± 79	28 ± 40	1540 ± 895	7.8 ± 4	108 ± 45	4
α1β2γ2S 1:1:1	13 ± 5	55 ± 45	72 ± 39	32 ± 41	1100 ± 880	13 ± 8	158 ± 137	6
α1β2γ2S 1:1:10	30 ± 13	81 ± 8	265 ± 137	18 ± 8	1711 ± 599	2 ± 1	106 ± 39	8
+GABARAP	16 ± 5	90 ± 8	162 ± 80	7 ± 7	1226 ± 470	4 ± 3	71 ± 46	6
αβtan+γ2S	19 ± 5	73 ± 19	125 ± 88	25 ± 19	1365 ± 560	2 ± 1	73 ± 27	4
+GABARAP	13 ± 6	89 ± 3	267 ± 155	5 ± 2	947 ± 345	6 ± 2	78 ± 16	3
αβtan+γ2L			48 ± 7	94 ± 1	1258 ± 448	6 ± 1	113 ± 15	3

αβtan+γ2S transfections may be attributable to occasional slight contamination by αβ receptors.

To further characterize receptors formed from tandem constructs, we examined their sensitivity to blockade by Zn^{2+}. Current block by Zn^{2+} was tested with 1 mM GABA, with or without 30 μM $ZnCl_2$ (Fig. 4). As expected, αβtan+α1 and α1β2 receptors were much more sensitive to Zn^{2+} block (mean ± SD; 89 ± 5 and 94 ± 2%, respectively) than αβtan+γ2S, αβtan+γ2L, or α1β2γ2S 1:1:10 receptors (13 ± 4, 11 ± 5, and 15 ± 5%, respectively).

GABA concentration responses were also measured for α1β2, α1β2γ2S 1:1:1, α1β2γ2S 1:1:10, αβtan+α1, and αβtan+γ2S transfections (Fig. 5). EC_{50} values were 5.6 ± 1.1 μM (mean ± SD) for α1β2 (Hill coefficient n_H, 1.30 ± 0.24), 7.8 ± 0.5 μM for αβtan+α1 (n_H 1.16 ± 0.05), 40.8 ± 8.8 μM for α1β2γ2S 1:1:10 (n_H 1.00 ± 0.08), and 46.6 ± 4.0 μM for αβtan+γ2S (n_H 1.16 ± 0.30). The average EC_{50} value for α1β2γ2S 1:1:1 was intermediate at 15.1 ± 7.9 with a Hill slope of 1.18 ± 0.08. EC_{50} values for α1β2 and αβtan+α1 were not significantly different from each other, nor were values for α1β2γ2S 1:1:10 and αβtan+γ2S. However, the EC_{50} value for α1β2γ2S 1:1:1 transfections was significantly different from all four of the other transfection types ($p < 0.001$). These findings are consistent with the kinetic data indicating that mixtures of αβ and αβγ receptors are formed in 1:1:1 transfections.

Estimations from mean-variance analysis yielded a peak open

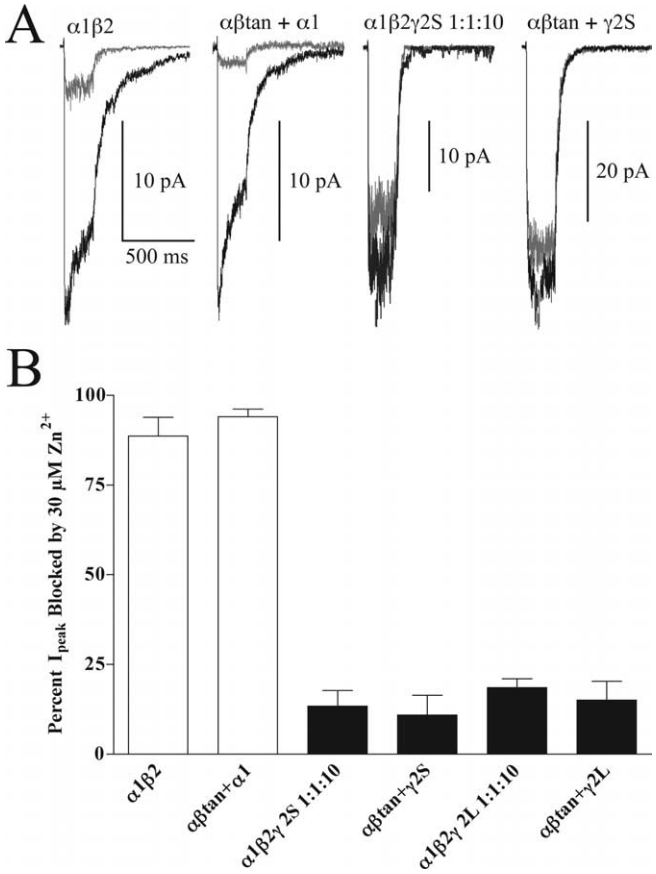

Figure 4. Zinc block of currents from transfections with $GABA_A$ receptor subunits and tandems. ***A***, Current traces from 200 ms 1 mM GABA pulses (black) superimposed with currents from the same patch exposed to a coapplication of 1 mM GABA plus 30 μM $ZnCl_2$ (gray) after equilibration in control solution plus 30 μM $ZnCl_2$. ***B***, Histograms for percentage of peak current blocked by Zn^{2+} for 200 ms GABA pulses. $\alpha1\beta2\gamma2S$ 1:1:10, $\alpha\beta$tan+$\gamma2S$, $\alpha\beta$tan+$\gamma2L$ 1:1:10, and $\alpha\beta$tan+$\gamma2L$ transfections (black bars) are significantly different ($p < 0.001$) from $\alpha1\beta2$ and $\alpha\beta$tan+α transfections (open bars). Data are mean ± SD (to show error) for 4–17 patches for each condition.

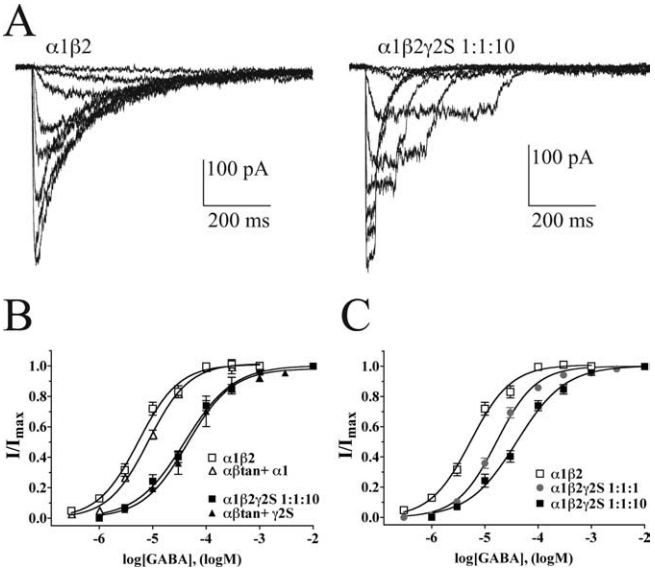

Figure 5. GABA concentration responses. ***A***, Current responses to increasing concentrations of GABA for $\alpha1\beta2$ transfections (with 0.3, 1.0, 3.0, 10, 30, 100, 300, and 1000 μM GABA) and $\alpha1\beta2\gamma2S$ 1:1:10 transfections (with 1, 3, 10, 30, 100, 300, 1000, and 3000 μM GABA). Pulse durations are described in Materials and Methods. Note that less desensitization occurs in $\alpha1\beta2\gamma2S$ 1:1:10 at any given concentration. ***B***, ***C***, Concentration–response curves and fits for $\alpha1\beta2$ and $\alpha\beta$tan+$\alpha1$ (open symbols) versus $\alpha1\beta2\gamma2S$ 1:1:10 and $\alpha\beta$tan+$\gamma2S$ (closed symbols) transfections (***B***) or $\alpha1\beta2\gamma2S$ 1:1:1 transfections (***C***, gray circles). Currents were normalized to a maximal response at a GABA concentration 10-fold higher than the curve-fit maximal responses shown. Data shown are means ± SEM for four or more patches each. In some cases, the error bars were smaller than the symbol for the mean. Note that 1 mM GABA is near-maximal for all combinations shown.

probability of 0.54 ± 0.05 (mean ± SD; $n = 3$ patches) for $\alpha1\beta2$, 0.56 ± 0.06 for $\alpha\beta$tan+$\alpha1$ ($n = 4$), 0.71 ± 0.10 for $\alpha1\beta2\gamma2S$ (1:1:10; $n = 7$), and 0.64 ± 0.05 for $\alpha\beta$tan+$\gamma2S$ receptors ($n = 3$ patches; data not shown). No significant differences were found between $\alpha1\beta2$ and $\alpha\beta$tan+$\alpha1$ receptors or between $\alpha1\beta2\gamma2S$ 1:1:10 and $\alpha\beta$tan+$\gamma2$ receptors. It should be noted that several patches for $\alpha1\beta2$ and $\alpha\beta$tan+$\alpha1$ receptors could not be fitted with the standard mean-variance equation (see Materials and Methods), which is poorly resolved below a value of 0.5. Thus, true open probability may be lower than 0.5 for $GABA_A$ receptors, as is reflected in other studies (Burkat et al., 2001; Mortensen et al., 2004).

Another difference between receptors that contain or lack a $\gamma2$ subunit is seen in their single-channel conductances (Angelotti and Macdonald, 1993). Figure 6 shows sample traces in which single openings were measured from transfections with $\alpha\beta$tan+$\alpha1$, $\alpha1\beta2$, $\alpha\beta$tan+$\gamma2S$, and $\alpha1\beta2\gamma2S$ 1:1:10. Conductances for either $\alpha\beta$tan+$\alpha1$ or $\alpha1\beta2$ receptors were ~15 pS with a ~10 pS subconductance, compared with ~29 pS (~21 pS subconductance) for $\alpha\beta$tan+$\gamma2S$ or $\alpha1\beta2\gamma2S$ 1:1:10 receptors.

If $\alpha1\beta2\gamma2S$ 1:1:1 transfections result in mixtures of $\alpha1\beta2$ and $\alpha1\beta2\gamma2S$ receptors, we would expect to see the 15 pS main conductance and 10 pS subconductance levels from $\alpha1\beta2$ receptors. Examining deactivating currents allowed detection of apparent $\alpha\beta$-like conductances from $\alpha1\beta2\gamma2S$ 1:1:1 transfections (Fig. 7). Figure 7*B* represents an example of a single $\alpha\beta$-like conductance observed under continuous 3 mM GABA exposure from an $\alpha1\beta2\gamma2S$ 1:1:1 transfection. Summaries of current–voltage plots and calculated chord conductances are shown for each of the five transfection types (Figs. 6, 7*C*). Note that we were able to observe all main and subconductance levels described in $\alpha1\beta2$ and $\alpha1\beta2\gamma2S$ 1:1:10 receptors in "mixed" $\alpha1\beta2\gamma2S$ 1:1:1 transfections (Fig. 7*C*).

GABARAP associates with γ subunits *in vivo* (Barnes, 2000; Nymann-Andersen et al., 2002a). Using GABARAP fused to EGFP as a reporter for expression, we found no effect of GABARAP-EGFP on desensitization or deactivation kinetics for $\alpha\beta$ transfections, as expected. However, we were surprised to observe no shifts in kinetics for $\alpha\beta$tan+$\gamma2S$ or $\alpha1\beta2\gamma2S$ 1:1:10 cotransfections with GABARAP-EGFP (Fig. 8*A–C*; Table 1, 2). We also saw no apparent change in single-channel amplitude with cotransfection of GABARAP-EGFP, dissimilar to a recent study of GABARAP effects (Everitt et al., 2004).

To investigate further the effects of GABARAP expression on $GABA_A$ receptor function, GABARAP-EGFP was cotransfected with $\alpha1\beta2\gamma2S$ 1:1:0.5. In this case, we observed a shift to slower and less extensive desensitization (Fig. 8*A*,*B*) and a concomitant reduction in the weighted time constant for deactivation following long (2000 ms) GABA pulses compared with $\alpha1\beta2\gamma2S$ 1:1:0.5 without added GABARAP-EGFP (Fig. 8*C*). Previous work has suggested that GABARAP association with $GABA_A$ receptors slows desensitization, speeds deactivation, and increases GABA EC_{50} values for $\alpha\beta\gamma$ receptors (Chen et al., 2000). These results suggest that GABARAP does not directly affect receptor kinetic properties but likely facilitates surface expression of $\alpha1\beta2\gamma2S$

receptors. This may occur by promoting $\gamma2S$ assembly into pentameric receptors by increasing $\alpha1\beta2\gamma2S$ receptor trafficking to the surface or by decreasing removal and degradation of surface $\alpha1\beta2\gamma2S$ receptors, thus shifting their kinetics and agonist properties toward more fully γ-incorporated populations.

We observed previously in oocytes that $\gamma2$ subunit overexpression reduces variability and increases the value for benzodiazepine-modulated potentiation of submaximal GABA currents (Boileau et al., 2002). We found here using mammalian cells that diazepam potentiation of I_{GABA} was quite variable for $\alpha1\beta2\gamma2S$ 1:1:0.5 transfections compared with $\alpha1\beta2\gamma2S$ 1:1:10 or $\alpha\beta$tan+$\gamma2S$ transfections (Fig. 8*D*). Cotransfection of GABARAP-EGFP had no significant effect on the potentiation values for $\alpha1\beta2\gamma2S$ 1:1:10 (2.0 ± 0.2; mean ± SD with GABARAP-EGFP vs 2.0 ± 0.2 without GABARAP-EGFP) or $\alpha\beta$tan+$\gamma2S$ transfections (2.3 ± 0.2 vs 2.4 ± 0.2) but increased the mean potentiation for $\alpha1\beta2\gamma2S$ 1:1:0.5 transfections from 1.1 ± 0.5 to 1.7 ± 0.3 ($p < 0.001$), corroborating our hypothesis of an increase in the ratio of surface $\alpha\beta\gamma$ to $\alpha\beta$ receptors.

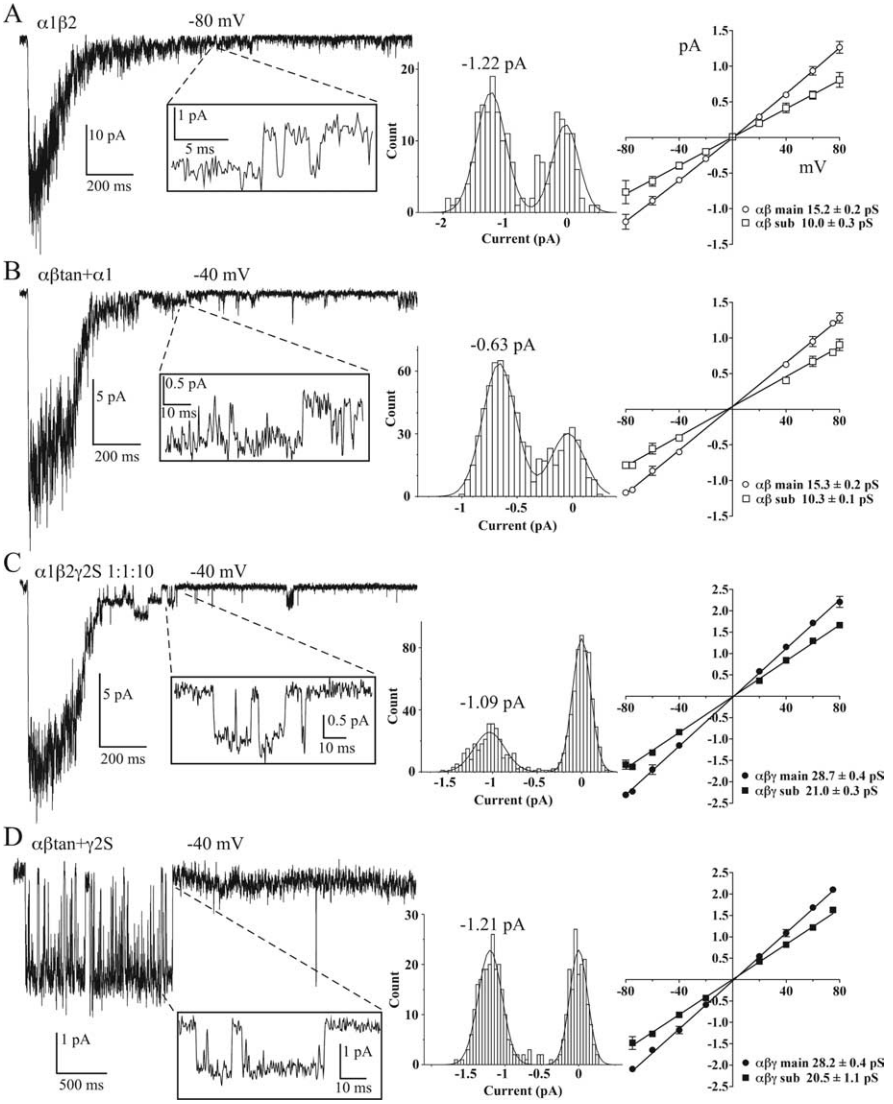

Figure 6. Single-channel openings and conductances. ***A–D***, Representative current traces for $\alpha1\beta2$ (***A***), $\alpha\beta$tan+$\alpha1$ (***B***), $\alpha1\beta2\gamma2S$ 1:1:10 (***C***), and $\alpha\beta$tan+$\gamma2S$ (***D***) transfections showing single-channel openings in tail currents after deactivation from a 200 ms, 10 mM GABA pulse or during the pulse in the case of ***D***. All points amplitude histograms (center) of the closed and open levels for the openings indicated (insets) and Gaussian fits. Current–voltage plots were constructed for each of the transfections (right). Calculated chord conductances are listed beneath each plot for main and subconductances. Data are mean ± SD from three or more patches.

Discussion

The majority of studies of expressed $GABA_A$ receptors have reported the characteristics for $\alpha\beta\gamma$ receptors expressed in a 1:1:1 or 1:1:0.5 ratio, which can have mixtures of $\alpha\beta$ and $\alpha\beta\gamma$ receptors (Boileau et al., 2002). Because the stoichiometry for the $\alpha\beta\gamma$ combination is likely to be 2:2:1 (Chang et al., 1996; Tretter et al., 1997), then a 1:1:1 mixture already contains a relative overexpression of the γ subunit. In this study, we constrained stoichiometry using tandem subunit concatamers to examine $GABA_A$ receptor macroscopic kinetics and pharmacology and demonstrate the utility of $\alpha1$-$\beta2$ tandem subunits for establishing the "intrinsic properties" of $\alpha1\beta2$ and $\alpha1\beta2\gamma2$ $GABA_A$ receptors. Using these tandem subunits, we could then interpret a mechanism by which GABARAP alters receptor kinetics.

α-β Tandems are capable of assembling into an appropriate pentamer with only free α or γ subunits. Expressing tandems alone or $\alpha\beta$tan+$\beta2$ in HEK293 cells yielded little or no current, suggesting that expression of $\alpha\beta$tan+$\gamma2$ or $\alpha\beta$tan+$\alpha1$ resulted in receptors with 2α:2β:1γ or 3α:2β pentamer stoichiometry, respectively. This contrasts with previous studies (Tretter et al., 1997; Horenstein et al., 2001) that suggested a 2α:3β stoichiometry for $\alpha\beta$ receptors. Thus, for $\alpha\beta$ receptors, it appears that both stoichiometries are possible and may even lead to receptors with similar characteristics. This warrants additional investigation. However, the structure of our tandem subunit, and/or the order of assembly allows for 3α:2β only and yields receptors that appear to be identical to free $\alpha1$ + $\beta2$ subunits. The lack of current produced by expressing tandem subunits alone or with the β subunit suggests that they do not produce monomers (Fig. 1) that can incorporate into receptors, nor do they "loop out" with only one of the two subunits incorporated into the pore-forming pentamer (Zhou et al., 2003; Groot-Kormelink et al., 2004). Furthermore, the similarity of $\alpha\beta$tan+$\gamma2$ to $\alpha1\beta2\gamma2$ 1:1:10 transfections suggests that the formation of both a functional $\alpha1$ and $\beta2$ subunit from a tandem subunit does not occur, because a mixture with $\alpha1\beta2$ receptors should be detectable in that case. Using a homology model of the $GABA_A$ receptor built using the ACh binding protein of *Lymnaea stagnalis* (Brejc et al., 2001) for the extracellular domain and the 4 Å structure of the nicotinic acetylcholine receptor (Unwin, 2005) for the transmembrane domains, a linker length of 33 amino acids is sufficient to traverse from the C terminus of the $\alpha1$ subunit to the N terminus of the $\beta2$ subunit at a $\beta2/\alpha1$ subunit interface (Minier and Sigel, 2004).

The desensitization characteristics of constrained $\alpha\beta\gamma$ recep-

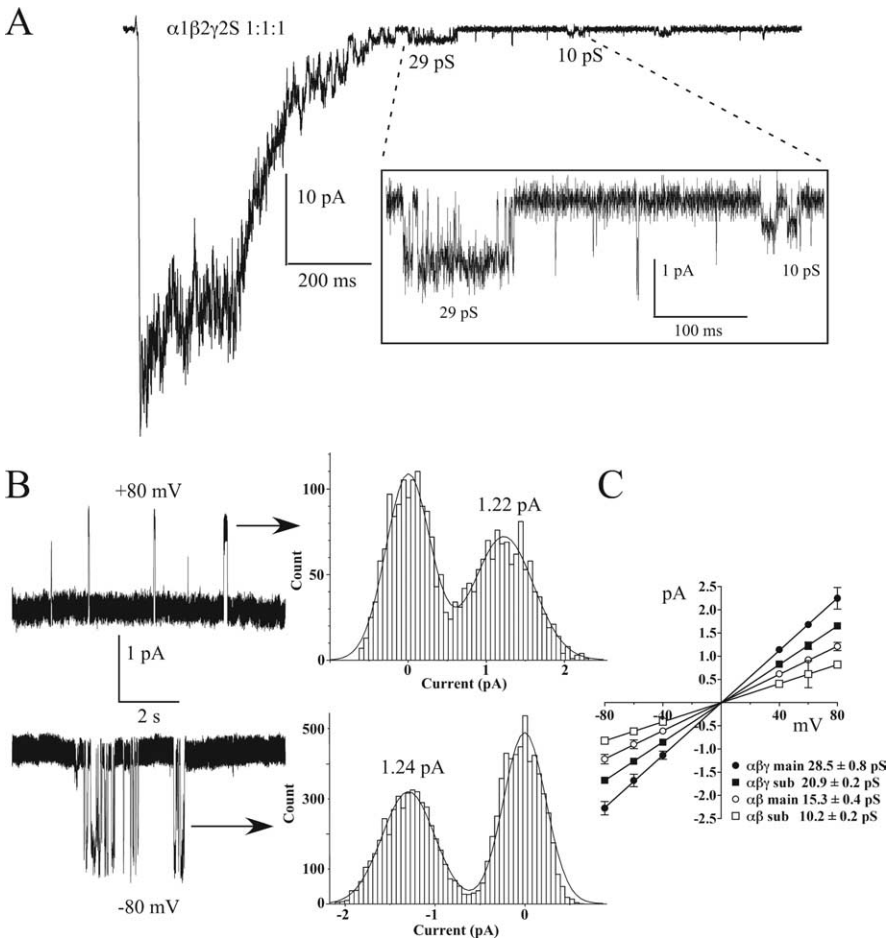

Figure 7. Single-channel conductances in $\alpha1\beta2\gamma2S$ 1:1:1 transfections. ***A***, Single-channel openings in tail currents after deactivation from a 200 ms, 10 mM GABA pulse with openings indicative of $\alpha\beta\gamma$ receptors (e.g., 29 pS) or $\alpha\beta$ receptors (e.g., 10 pS, inset). ***B***, Clusters of single openings from an excised patch held at ± 80 mV. Amplitude histograms (center) of the closed and open levels for the clusters indicated (arrows) and Gaussian fits yielding ~15 pS chord conductance are shown, consistent with $\alpha\beta$ receptors. ***C***, Current–voltage plots were constructed for each of the transfections (right), culled from seven patches from six different transfections in which single-channel openings were detectable. Calculated chord conductances are listed beneath the plot for main and subconductances (sub). Data are mean ± SD.

tors differ greatly from $\alpha\beta$ receptors (Figs. 1–3; Table 1). The weighted time constant of desensitization increases significantly as the γ ratio is increased (Fig. 3*A*, Table 1). The percentage of current remaining at the ends of 2 s GABA pulses can be also used as a hallmark to distinguish $\alpha\beta\gamma$ receptors ($\alpha\beta$tan+$\gamma2$, $\alpha1\beta2\gamma2S$ 1:1:10) from $\alpha\beta$ receptors ($\alpha\beta$tan+$\alpha1$, $\alpha1\beta2$) (Fig. 3*B*). Usually when the γ subunit is overexpressed, or in all cases of $\alpha\beta$tan+$\gamma2$ transfections, there are no discernable fast (~25 ms, ~150 ms) components of desensitization (Figs. 1–3, Table 1). This is reminiscent of coexpression of the δ subunit with α and β subunits (Haas and Macdonald, 1999; Bianchi et al., 2001). The faster deactivation in $\alpha\beta\gamma$ receptors compared with $\alpha\beta$ receptors (Fig. 3*C*, Table 2) is consistent with the concomitant slowed desensitization, according to the hypothesis that deactivation is prolonged by bound, desensitized receptors visiting an open state before agonist unbinding occurs (Jones and Westbrook, 1995).

We also observed a rightward shift in the GABA concentration response for $\alpha1\beta2\gamma2S$ receptors (EC_{50}, 40.8 ± 8.8 μM), compared with $\alpha1\beta2$ receptors (EC_{50}, 5.6 ± 1.1 μM), with no difference in Hill slopes (Fig. 5). Transfection with $\alpha\beta$tan+$\alpha1$ (EC_{50}, 7.8 ± 0.5 μM) was again very similar to $\alpha1\beta2$, and $\alpha\beta$tan+$\gamma2S$ (EC_{50}, 46.6 ± 4.0 μM) was indistinguishable from $\alpha1\beta2\gamma2S$ 1:1:10 in this measure. Blockade by Zn^{2+} also demonstrated that tandem subunits respond similarly to "free" $\alpha1\beta2$ and $\alpha1\beta2\gamma2S$ 1:1:10 transfections (Fig. 4).

One of the characteristic differences between $\alpha\beta$ and $\alpha\beta\gamma$ receptors measured was channel conductance. Consistent with previous studies (Verdoorn et al., 1990; Angelotti and Macdonald, 1993), $\alpha\beta$tan+$\alpha1$ receptors showed a 15 pS main conductance and a 10 pS subconductance, as did receptors from $\alpha1\beta2$ transfections. The conductance levels for both $\alpha\beta$tan+$\gamma2$ and $\alpha1\beta2\gamma2$ 1:1:10 transfections were 29 and 21 pS, also consistent with those reported previously (Angelotti and Macdonald, 1993; Angelotti et al., 1993; Mortensen et al., 2004). Discerning single "contaminating" $\alpha\beta$ channels that might exist in a 1:1:1 α:β:γ mixture can be made more difficult by receptor clustering making single-channel patches a relative rarity, smaller $\alpha\beta$ conductances, and higher levels of desensitization in $\alpha\beta$ receptors (Figs. 1, 2) under continuous GABA application. By examining deactivating currents (Fig. 6), we were able to discern both $\alpha\beta$ and $\alpha\beta\gamma$ conductance levels in $\alpha1\beta2\gamma2$ 1:1:1 transfections. There have been some observations of $\alpha\beta$-like conductances in heterologous expression systems (Angelotti and Macdonald, 1993; Mortensen et al., 2004) and in native preparations (Brickley et al., 1999). However, neuronal cells also contain receptors that consist of different subunit subtypes than those used here.

The effects of fixed $\gamma2$ subunit incorporation on desensitization, deactivation, and GABA sensitivity are strikingly similar to the effects that were observed when the receptor-associated protein GABARAP was cotransfected with $\alpha1$, $\beta2$, and $\gamma2L$ subunits in QT-6 quail fibroblasts (Chen et al., 2000). In that case, desensitization was slowed, deactivation was accelerated, and the GABA concentration response was shifted to the right. Chen et al. (2000) hypothesized that these effects resulted from $GABA_A$ receptor clustering induced by GABARAP. A possible alternative explanation for these changes is that GABARAP facilitates surface expression of $\alpha1\beta2\gamma2S$ receptors and results in a more homogeneous population of $\alpha\beta\gamma$ receptors. Our results are most consistent with this alternative hypothesis (Fig. 8), because cotransfection with GABARAP-EGFP did not alter the macroscopic kinetics of $\alpha1\beta2\gamma2S$ 1:1:10 or $\alpha\beta$tan+$\gamma2S$ transfections, whereas $\alpha1\beta2\gamma2S$ 1:1:0.5 mixed receptor populations were shifted in desensitization and deactivation to values closer to constrained $\alpha\beta\gamma$ receptors.

In addition, the presence of GABARAP increased diazepam potentiation of I_{GABA} for $\alpha1\beta2\gamma2S$ 1:1:0.5 transfections at subsaturating GABA concentrations (Fig. 8*D*), suggesting a decrease in the relative proportion of $\alpha\beta$ receptors in the mixture. Perhaps GABARAP aids in $\alpha\beta\gamma$ receptor trafficking to the surface via its association with the γ subunit, promotes $\gamma2S$ assembly into receptors, or reduces $\alpha\beta\gamma$ receptor turnover. Recently, Chen et al.

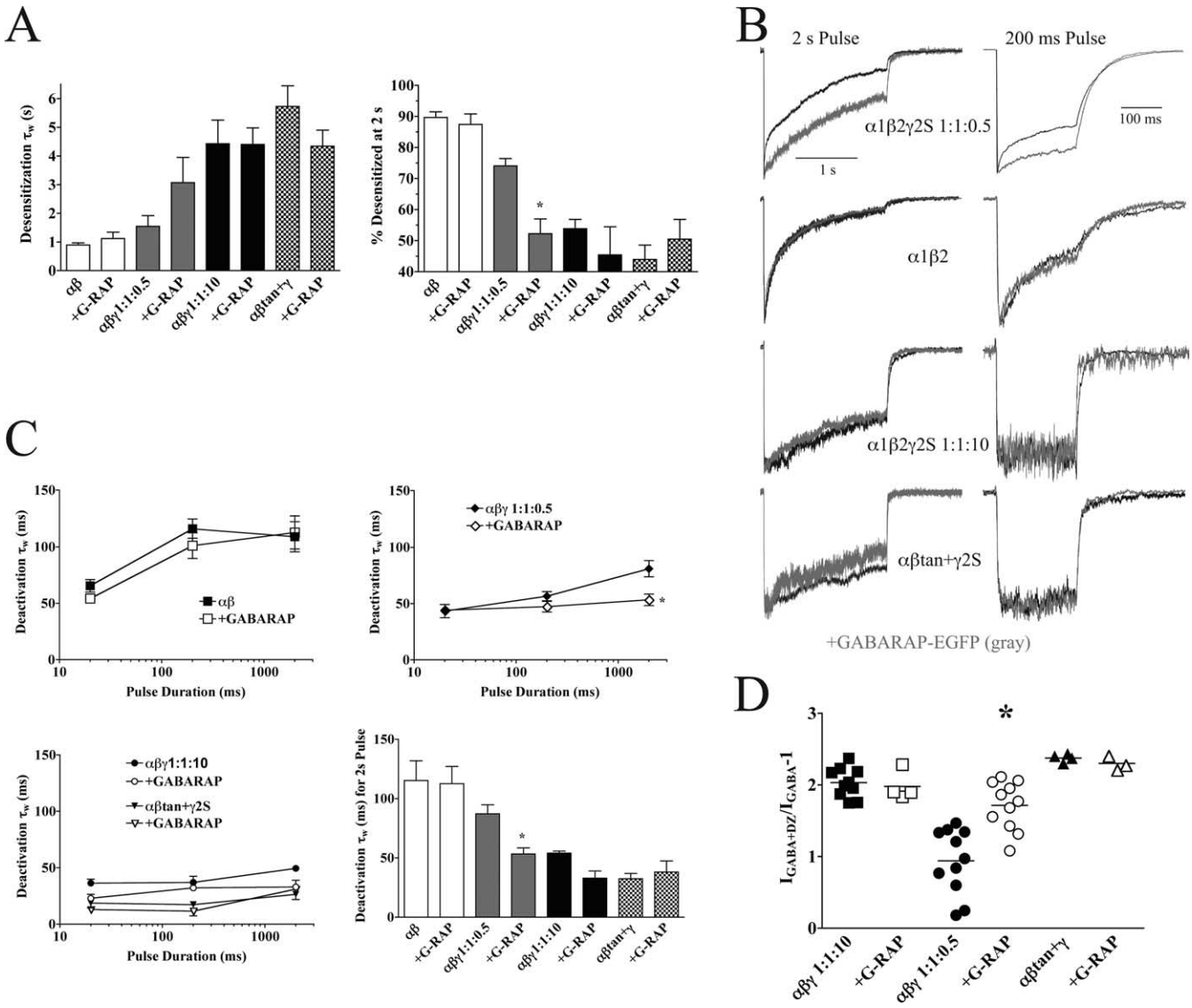

Figure 8. Coexpression of GABA$_A$ subunits with a GABARAP-EGFP fusion protein. ***A***, Summary of effects of GABARAP-EGFP on desensitization. Desensitization weighted time constants (τ_w) for each of the transfection types are shown in the left panel, compared with the extent of desensitization in the right panel. Data are mean ± SEM. The asterisk denotes significant difference from the non-GABARAP transfection at $p < 0.01$. ***B***, Representative current traces (black traces) of $\alpha1\beta2\gamma2S$ 1:1:0.5 (top), $\alpha1\beta2$ (second row), $\alpha1\beta2\gamma2S$ 1:1:10 (third row), and $\alpha\beta$tan+$\gamma2S$ transfections (bottom) overlaid with current traces from the same subunits cotransfected with GABARAP-EGFP (gray traces). GABA pulse durations shown are 2000 ms (left) to show changes in desensitization and 200 ms (right) to show changes in deactivation. ***C***, Summary of effects of GABARAP-EGFP on deactivation. Deactivation weighted time constants (τ_w) following GABA pulses of 20, 200, and 2000 ms duration are shown for $\alpha\beta$ (top left panel), $\alpha1\beta2\gamma2S$ 1:1:0.5 (top right), $\alpha1\beta2\gamma2S$ 1:1:10, and $\alpha\beta$tan+$\gamma2S$ transfections (bottom left) with (closed symbols) and without (open symbols) coexpression of GABARAP-EGFP. The bottom right panel summarizes data for the 2000 ms GABA pulse. Data are mean ± SEM. The asterisk denotes significant difference from the non-GABARAP transfection at $p < 0.05$. ***D***, Effects of cotransfection of GABARAP-EGFP on diazepam-induced potentiation of subsaturating GABA responses. Each point represents data from one patch pulsed for 500 ms with 3 μM GABA for several sweeps and then equilibrated in 1 μM DZ and pulsed with 3 μM GABA plus 1 μM DZ. Peak currents were measured preincubation and postincubation with DZ, and potentiation was calculated as follows: $I_{GABA+DZ}/I_{GABA} - 1$. Horizontal lines represent the mean. The asterisk denotes significant difference from the non-GABARAP transfection at $p < 0.001$. G-RAP, GABARAP.

(2005) observed increased surface expression of $\alpha1\beta2\gamma2S$ receptors in *Xenopus* oocyte expression and showed that microtubule-binding domains of GABARAP were required for the effect. They expressed subunits in a 1:1:2 α:β:γ ratio (thus, a moderate overexpression of γ subunits) and therefore saw no changes in GABA EC_{50} or benzodiazepine responses after addition of GABARAP.

To make predictions about the kinetic behavior of $\alpha\beta$ and $\alpha\beta\gamma$ receptor mixtures, we developed simplified kinetic models that simulate currents from $\alpha\beta$tan+$\alpha1$ and $\alpha\beta$tan+$\gamma2S$ receptors (Fig. 9). We then averaged simulated currents from the two models to predict what percentage of $\alpha\beta\gamma$ receptors might be present in preparations that are not fixed in stoichiometry (Fig. 9*C*). The variability in both desensitization and deactivation observed in $\alpha\beta\gamma$ 1:1:1 transfections (Fig. 9*D*) can be modeled with mixtures of $\alpha\beta$tan+$\alpha1$ and $\alpha\beta$tan+$\gamma2S$ receptors in a ratio ranging from 3:1 to 1:1, respectively (Fig. 9*C*). Using these models and the measured weighted desensitization time constants (Table 1) and percentages of desensitization at the end of 2 s 10 mM GABA pulses (Fig. 8), we predict that there is an approximate doubling of the percentage of $\alpha\beta\gamma$ receptors in $\alpha1\beta2\gamma2S$ 1:1:0.5 transfections in the presence of GABARAP.

Another way to estimate percentage of $\alpha\beta\gamma$ receptors in a mixture is to measure benzodiazepine potentiation. Modeling

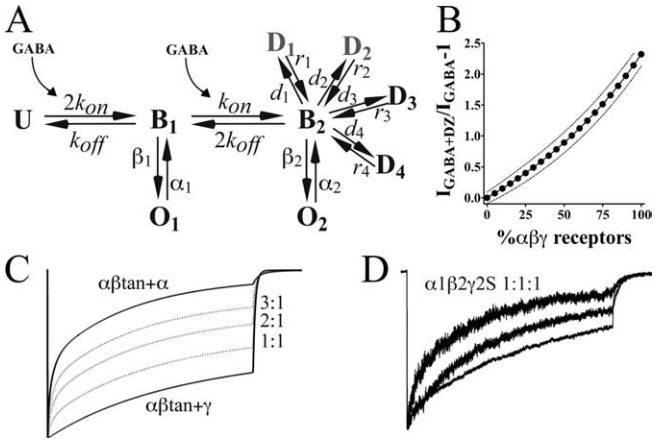

Figure 9. Model of currents for $\alpha\beta$ receptors compared with $\alpha\beta\gamma$ receptors. ***A***, Kinetic scheme. Using a backbone kinetic model with one unbound (U) state, single-liganded (B1) and double-liganded (B2) states, and an open state (O_1, O_2) from each of the liganded states (Jones and Westbrook, 1995; Hinkle and Macdonald, 2003), currents for $\alpha\beta$tan+α1 versus $\alpha\beta$tan+γ2S were simulated (see Materials and Methods). Parameters optimized were desensitization and deactivation time constants, apparent affinity (EC_{50}), and open probability for macroscopic currents. A simplified model for $\alpha\beta$tan+α1 ($\alpha\beta$) receptors had the following rates: k_{on}, 5×10^6 M^{-1} s^{-1}; k_{off}, 100 s^{-1}; β1 (B1 to O1), 200 s^{-1}; α1 (O1 to B1), 1100 s^{-1}; β2, 1800 s^{-1}; α2, 280 s^{-1}. The model for $\alpha\beta$tan+γ2S ($\alpha\beta\gamma$) receptors used the following rates: k_{on}, 5×10^4 M^{-1} s^{-1}; k_{off}, 200 s^{-1}; β1 (B1 to O1), 50 s^{-1}; α1 (O1 to B1), 3100 s^{-1}; β2, 1800 s^{-1}; α2, 280 s^{-1}. Both models differ dramatically in their desensitization (d) and recovery (r) rates. For $\alpha\beta$tan+α1 receptors, faster entry desensitized states (D1, D2, gray) were connected to B2 with the following rates: $d1$, 200 s^{-1}; $r1$, 80 s^{-1}; $d2$, 60 s^{-1}; $r2$, 12 s^{-1}. Slower entry D states (D3, D4) were modeled with the following rates: $d3$, 12 s^{-1}; $r3$, 0.03 s^{-1}; $d4$, 6 s^{-1}; $r4$, 0.3 s^{-1}. For the two relatively slow desensitizing components seen in $\alpha\beta$tan+γ2S currents (also designated D3 and D4), the rates were as follows: $d3$, 2 s^{-1}; $r3$, 0.75 s^{-1}; $d4$, 1 s^{-1}; $r4$, 0.05 s^{-1}. ***B***, Model of diazepam potentiation for varying amounts of $\alpha\beta$ and $\alpha\beta\gamma$ receptors in a mixture. Experimentally determined values for maximal diazepam potentiation ($I_{GABA+DZ}/I_{GABA} - 1$), EC_{50}, open probability, and conductance for both $\alpha\beta$ and $\alpha\beta\gamma$ receptors were used to generate the curve of expected values and 95% confidence intervals (see Materials and Methods). ***C***, Simulated model traces for $\alpha\beta$tan+α1 and $\alpha\beta$tan+γ2S (bold), with averaged traces generated from mixtures of $\alpha\beta$tan+α1 and $\alpha\beta$tan+γ2S receptors in a 3:1, 2:1, and 1:1 $\alpha\beta$tan+α1:$\alpha\beta$tan+γ2S ratio (dotted line). ***D***, Traces from three excised patches from cells transected at a 1:1:1 α1:β2:γ2S ratio, showing variability in macroscopic kinetics.

the maximal benzodiazepine potentiation expected in a mixture of $\alpha\beta$ and $\alpha\beta\gamma$ receptors at 3 μM GABA (Fig. 8*D*), we calculate that the percentage of $\alpha\beta\gamma$ receptors in our $\alpha1\beta2\gamma2$S 1:1:0.5 transfections ranges from 14–69%. In the presence of GABARAP-EGFP, this increases to a range of 54–88% $\alpha\beta\gamma$ receptors, approximately doubling, similar to our kinetic modeling prediction. Thus, the amount of benzodiazepine potentiation is a straightforward predictor of the percentage of $\alpha\beta\gamma$ receptors in a patch.

Clusters of γ-containing $GABA_A$ receptors are found at synapses (Sassoe-Pognetto and Fritschy, 2000; Brunig et al., 2002; Christie et al., 2002) and are thought to mediate so-called "phasic" inhibition (Farrant and Nusser, 2005). Some GABAergic synapses may not contain fast-desensitizing receptors (Kraushaar and Jonas, 2000; Mellor and Randall, 2001), although in other studies, it has been suggested that desensitization of postsynaptic receptors shapes IPSC kinetics and responses to repetitive stimulation (Jones and Westbrook, 1995, 1996; Pearce et al., 1995; Overstreet et al., 2000). Thus, our finding that incorporation of a γ subunit produces receptors that do not undergo rapid desensitization presents an apparent contradiction. One possible explanation is that mixtures of $\alpha\beta$ and $\alpha\beta\gamma$ exist at synapses, the $\alpha\beta$ receptors accounting for desensitization and $\alpha\beta\gamma$ receptors for benzodiazepine sensitivity. There is some suggestive evidence for the existence of $\alpha\beta$ receptors in developing neurons (Brickley et al., 1999). Alternatively, γ-containing receptors may undergo rapid desensitization at synapses, but the HEK293 cell heterologous expression system may not faithfully reproduce the kinetic properties of neuronal receptors, which are subject to the influence of phosphorylation and additional modulatory factors. Although we are unable to distinguish between these possibilities at the present time, because the exact mixture of subunits and subunit subtypes is difficult to measure in isolated synapses, future studies that address this issue should benefit from the characterization of pharmacological and physiological properties of homogeneous receptor populations using tandem subunits and other techniques that we describe here.

References

Angelotti TP, Macdonald RL (1993) Assembly of $GABA_A$ receptor subunits: $\alpha1\beta1$ and $\alpha1\beta1\gamma2$S subunits produce unique ion channels with dissimilar single-channel properties. J Neurosci 13:1429–1440.

Angelotti TP, Uhler MD, Macdonald RL (1993) Assembly of $GABA_A$ receptor subunits: analysis of transient single-cell expression utilizing a fluorescent substrate/marker gene technique. J Neurosci 13:1418–1428.

Barnard EA, Skolnick P, Olsen RW, Mohler H, Sieghart W, Biggio G, Braestrup C, Bateson AN, Langer SZ (1998) International Union of Pharmacology. XV. Subtypes of gamma-aminobutyric acidA receptors: classification on the basis of subunit structure and receptor function. Pharmacol Rev 50:291–313.

Barnes Jr EM (2000) Intracellular trafficking of GABA(A) receptors. Life Sci 66:1063–1070.

Baumann SW, Baur R, Sigel E (2001) Subunit arrangement of gamma-aminobutyric acid type A receptors. J Biol Chem 276:36275–36280.

Baumann SW, Baur R, Sigel E (2002) Forced subunit assembly in alpha1beta2gamma2 $GABA_A$ receptors. Insight into the absolute arrangement. J Biol Chem 277:46020–46025.

Benke D, Mertens S, Trzeciak A, Gillessen D, Mohler H (1991) $GABA_A$ receptors display association of gamma 2-subunit with alpha 1- and beta 2/3-subunits. J Biol Chem 266:4478–4483.

Benke D, Fritschy JM, Trzeciak A, Bannwarth W, Mohler H (1994) Distribution, prevalence, and drug binding profile of gamma-aminobutyric acid type A receptor subtypes differing in the beta-subunit variant. J Biol Chem 269:27100–27107.

Benkwitz C, Banks MI, Pearce RA (2004) Influence of $GABA_A$ receptor gamma2 splice variants on receptor kinetics and isoflurane modulation. Anesthesiology 101:924–936.

Bianchi MT, Macdonald RL (2002) Slow phases of GABA(A) receptor desensitization: structural determinants and possible relevance for synaptic function. J Physiol (Lond) 544:3–18.

Bianchi MT, Haas KF, Macdonald RL (2001) Structural determinants of fast desensitization and desensitization-deactivation coupling in $GABA_A$ receptors. J Neurosci 21:1127–1136.

Boileau AJ, Czajkowski C (1999) Identification of transduction elements for benzodiazepine modulation of the $GABA_A$ receptor: three residues are required for allosteric coupling. J Neurosci 19:10213–10220.

Boileau AJ, Baur R, Sharkey LM, Sigel E, Czajkowski C (2002) The relative amount of cRNA coding for gamma2 subunits affects stimulation by benzodiazepines in $GABA_A$ receptors expressed in *Xenopus* oocytes. Neuropharmacology 43:695–700.

Boileau AJ, Li T, Benkwitz C, Czajkowski C, Pearce RA (2003) Effects of gamma2S subunit incorporation on $GABA_A$ receptor macroscopic kinetics. Neuropharmacology 44:1003–1012.

Bonnert TP, McKernan RM, Farrar S, le Bourdelles B, Heavens RP, Smith DW, Hewson L, Rigby MR, Sirinathsinghji DJ, Brown N, Wafford KA, Whiting PJ (1999) theta, a novel gamma-aminobutyric acid type A receptor subunit. Proc Natl Acad Sci USA 96:9891–9896.

Brejc K, van Dijk WJ, Klaassen RV, Schuurmans M, van Der Oost J, Smit AB, Sixma TK (2001) Crystal structure of an ACh-binding protein reveals the ligand-binding domain of nicotinic receptors. Nature 411:269–276.

Brickley SG, Cull-Candy SG, Farrant M (1999) Single-channel properties of synaptic and extrasynaptic $GABA_A$ receptors suggest differential targeting of receptor subtypes. J Neurosci 19:2960–2973.

Brunig I, Scotti E, Sidler C, Fritschy JM (2002) Intact sorting, targeting, and clustering of gamma-aminobutyric acid A receptor subtypes in hippocampal neurons in vitro. J Comp Neurol 443:43–55.

Burkat PM, Yang J, Gingrich KJ (2001) Dominant gating governing transient $GABA_A$ receptor activity: a first latency and Po/o analysis. J Neurosci 21:7026–7036.

Chang Y, Wang R, Barot S, Weiss DS (1996) Stoichiometry of a recombinant $GABA_A$ receptor. J Neurosci 16:5415–5424.

Chen L, Wang H, Vicini S, Olsen RW (2000) The gamma-aminobutyric acid type A ($GABA_A$) receptor-associated protein (GABARAP) promotes $GABA_A$ receptor clustering and modulates the channel kinetics. Proc Natl Acad Sci USA 97:11557–11562.

Christie SB, Li RW, Miralles CP, Riquelme R, Yang BY, Charych E, Wendou Y, Daniels SB, Cantino ME, De Blas AL (2002) Synaptic and extrasynaptic $GABA_A$ receptor and gephyrin clusters. Prog Brain Res 136:157–180.

Everitt AB, Luu T, Cromer B, Tierney ML, Birnir B, Olsen RW, Gage PW (2004) Conductance of recombinant GABA(A) channels is increased in cells co-expressing GABA(A) receptor-associated protein. J Biol Chem 279:21701–21706.

Farrant M, Nusser Z (2005) Variations on an inhibitory theme: phasic and tonic activation of GABA(A) receptors. Nat Rev Neurosci 6:215–229.

Graham FL, van der Eb AJ (1973) Transformation of rat cells by DNA of human adenovirus 5. Virology 54:536–539.

Groot-Kormelink PJ, Broadbent SD, Boorman JP, Sivilotti LG (2004) Incomplete incorporation of tandem subunits in recombinant neuronal nicotinic receptors. J Gen Physiol 123:697–708.

Günther U, Benson J, Benke D, Fritschy J-M, Reyes G, Knoflach F, Crestani F, Aguzzi A, Arigoni M, Lang Y, Bluethmann H, Mohler H, Lüscher B (1995) Benzodiazepine-insensitive mice generated by targeted disruption of the gamma 2 subunit gene of gamma-aminobutyric acid type A receptors. Proc Natl Acad Sci USA 92:7749–7753.

Haas KF, Macdonald RL (1999) $GABA_A$ receptor subunit gamma2 and delta subtypes confer unique kinetic properties on recombinant $GABA_A$ receptor currents in mouse fibroblasts. J Physiol (Lond) 514:27–45.

Hevers W, Luddens H (1998) The diversity of $GABA_A$ receptors. Pharmacological and electrophysiological properties of $GABA_A$ channel subtypes. Mol Neurobiol 18:35–86.

Hinkle DJ, Macdonald RL (2003) β Subunit phosphorylation selectively increases fast desensitization and prolongs deactivation of $\alpha1\beta1\gamma2$L and $\alpha1\beta3\gamma2$L $GABA_A$ receptor currents. J Neurosci 23:11698–11710.

Horenstein J, Wagner DA, Czajkowski C, Akabas MH (2001) Protein mobility and GABA-induced conformational changes in GABA(A) receptor pore-lining M2 segment. Nat Neurosci 4:477–485.

Im WB, Pregenzer JF, Binder JA, Dillon GH, Alberts GL (1995) Chloride channel expression with the tandem construct of alpha 6-beta 2 $GABA_A$ receptor subunit requires a monomeric subunit of alpha 6 or gamma 2. J Biol Chem 270:26063–26066.

Jones MV, Westbrook GL (1995) Desensitized states prolong $GABA_A$ channel responses to brief agonist pulses. Neuron 15:181–191.

Jones MV, Westbrook GL (1996) The impact of receptor desensitization on fast synaptic transmission. Trends Neurosci 19:96–101.

Kofuji P, Wang JB, Moss SJ, Huganir RL, Burt DR (1991) Generation of two forms of the gamma-aminobutyric acidA receptor gamma 2-subunit in mice by alternative splicing. J Neurochem 56:713–715.

Kraushaar U, Jonas P (2000) Efficacy and stability of quantal GABA release at a hippocampal interneuron-principal neuron synapse. J Neurosci 20:5594–5607.

Laurie DJ, Seeburg PH, Wisden W (1992) The distribution of 13 $GABA_A$ receptor subunit mRNAs in the rat brain. II. Olfactory bulb and cerebellum. J Neurosci 12:1063–1076.

Mellor JR, Randall AD (2001) Synaptically released neurotransmitter fails to desensitize postsynaptic GABA(A) receptors in cerebellar cultures. J Neurophysiol 85:1847–1857.

Mercik K, Pytel M, Mozrzymas JW (2003) Recombinant alpha 1 beta 2 gamma 2 GABA(A) receptors expressed in HEK293 and in QT6 cells show different kinetics. Neurosci Lett 352:195–198.

Minier F, Sigel E (2004) Techniques: use of concatenated subunits for the study of ligand-gated ion channels. Trends Pharmacol Sci 25:499–503.

Mohler H, Knoflach F, Paysan J, Motejlek K, Benke D, Luscher B, Fritschy JM (1995) Heterogeneity of GABAA-receptors: cell-specific expression, pharmacology, and regulation. Neurochem Res 20:631–636.

Mortensen M, Kristiansen U, Ebert B, Frolund B, Krogsgaard-Larsen P, Smart TG (2004) Activation of single heteromeric GABA(A) receptor ion channels by full and partial agonists. J Physiol (Lond) 557:389–413.

Nymann-Andersen J, Sawyer GW, Olsen RW (2002a) Interaction between $GABA_A$ receptor subunit intracellular loops: implications for higher order complex formation. J Neurochem 83:1164–1171.

Nymann-Andersen J, Wang H, Chen L, Kittler JT, Moss SJ, Olsen RW (2002b) Subunit specificity and interaction domain between GABA(A) receptor-associated protein (GABARAP) and GABA(A) receptors. J Neurochem 80:815–823.

Overstreet LS, Jones MV, Westbrook GL (2000) Slow desensitization regulates the availability of synaptic GABA(A) receptors. J Neurosci 20:7914–7921.

Pearce RA, Grunder SD, Faucher LD (1995) Different mechanisms for use-dependent depression of two $GABA_A$-mediated IPSCs in rat hippocampus. J Physiol (Lond) 484:425–435.

Sassoe-Pognetto M, Fritschy JM (2000) Mini-review: gephyrin, a major postsynaptic protein of GABAergic synapses. Eur J Neurosci 12:2205–2210.

Stephenson FA (1995) The $GABA_A$ receptors. Biochem J 310:1–9.

Traynelis SF, Silver RA, Cull-Candy SG (1993) Estimated conductance of glutamate receptor channels activated during EPSCs at the cerebellar mossy fiber-granule cell synapse. Neuron 11:279–289.

Tretter V, Ehya N, Fuchs K, Sieghart W (1997) Stoichiometry and assembly of a recombinant $GABA_A$ receptor subtype. J Neurosci 17:2728–2737.

Trussell LO, Fischbach GD (1989) Glutamate receptor desensitization and its role in synaptic transmission. Neuron 3:209–218.

Unwin N (2005) Refined structure of the nicotinic acetylcholine receptor at 4Å resolution. J Mol Biol 346:967–989.

Verdoorn TA, Draguhn A, Ymer S, Seeburg PH, Sakmann B (1990) Functional properties of recombinant rat $GABA_A$ receptors depend upon subunit composition. Neuron 4:919–928.

Vicini S (1991) Pharmacologic significance of the structural heterogeneity of the GABAA receptor-chloride ion channel complex. Neuropsychopharmacology 4:9–15.

Vicini S (1999) New perspectives in the functional role of GABA(A) channel heterogeneity. Mol Neurobiol 19:97–110.

Yeh HH, Grigorenko EV (1995) Deciphering the native $GABA_A$ receptor: is there hope? J Neurosci Res 41:567–571.

Zhou Y, Nelson ME, Kuryatov A, Choi C, Cooper J, Lindstrom J (2003) Human $\alpha4\beta2$ acetylcholine receptors formed from linked subunits. J Neurosci 23:9004–9015.